01,05

The Formation of the Structure and Magnetic Properties of $Sm_2Fe_{17}C_x$ Powders with Zn Additives Obtained by Mechanosynthesis

© V.A. Mikheev, E.S. Savchenko, E.V. Argunov, A.I. Novikov, I.V. Shchetinin

University of Science and Technology "MISIS",

Moscow, Russia

E-mail: vmikheev@misis.ru Received March 6, 2025 Revised March 6, 2025 Accepted May 5, 2025

The formation is investigated of the structure and magnetic properties of powders of $Sm_2Fe_{17}C_x$ (a $Sm_2Fe_{17}N_x$ -related compound) with Zn additives obtained by mechanosynthesis. The powders were examined by X-ray diffraction, scanning electron microscopy, and vibrating sample magnetometry. We found that a stage of mechanosynthesis prior to annealing is still necessary for obtaining the compound $Sm_2Fe_{17}C_x$ with high hysteresis properties despite the use of carbon nanotubes as a carbon-bearing additive. After annealing, the formation of the following Zn-containing phases was observed: Fe_3Zn_{10} ($I\bar{4}3m$) and Sm_2Zn_{17} ($R\bar{3}m$) in the annealing temperature range of 350–375 and 400–450 °C, respectively. The temperature of active decomposition of the $Sm_2Fe_{17}C_x$ phase for a mixture with Zn was 50 °C higher than that for a mixture without Zn. The increase of annealing temperature enhanced the specific saturation magnetization of the samples but decreased the coercivity.

Keywords: Sm₂Fe₁₇, Sm-Fe-C, Sm₂Fe₁₇C_x, carbon nanotubes, mechanochemical synthesis.

DOI: 10.61011/PSS.2025.06.61702.15HH-25

1. Introduction

Extensively growing alternative energy sector drives the demand for permanent magnets that are used in motors and power generator [1–4]. Permanent magnets with maximum magnetic energy density are currently fabricated using expensive rare-earth compounds and 3d-metals based on Sm-Co and Nd-Fe-B systems. Cheaper permanent magnets made of ferrite materials have lower magnetic energy densities [5,6]. Development of low-cost materials for permanent magnets with properties exceeding those of ferrite magnets is a critical task [7,8].

Sm-Fe-N is one of such promising systems because the $\rm Sm_2Fe_{17}N_x$ compound has the highest theoretical maximum magnetic energy product among the known systems [9]. $\rm Sm_2Fe_{17}N_x$ have a set of other advantages over $\rm Nd_2Fe_{14}B$: higher Curie temperature an magnetocrystalline anisotropy constant, the absence of spin-reorientation transition at negative temperatures, higher oxidation resistance (no coating is required), lower rare-earth metal (REM) concentration and lower cost of Sm compared with other REM (including Nd, Tb and Dy) [10–12] used for Nd-Fe-B magnet fabrication. However, the gas-phase method for preparing $\rm Sm_2Fe_{17}N_x$ is a resource-intensive technique (nitrogenation takes $\rm 20-40\,h$), often poorly repeatable, and also implies potential harmful nitrogen gas emission [13].

 $Sm_2Fe_{17}C_x$ is a direct alternative of $Sm_2Fe_{17}N_x$ with identical structure and inherits all advantages of the latter, while is free of the above-mentioned drawbacks [14]. This compound may be prepared using solid-phase methods such as, for example, mechanical synthesis [15]. Advantages

of the mechanical synthesis include not only ability to prepare nanopowders with high hysteresis properties, but also potential scaling up for industrial applications [16,17].

Process-related difficulties are encountered when preparing bulk magnets from Sm₂Fe₁₇C_x powders. Classical hot-pressing sintering method at temperatures higher than 1100 °C is not suitable for Sm₂Fe₁₇C_x because this compound decomposes at temperatures higher than 512 °C [18]. Spark plasma sintering was considered as one of possible solutions to this problem where sintering is performed at lower temperatures by providing local heating in contact points between particles, however, this method may be difficult to use in industrial applications [19]. High-pressure torsion method may be also used to prepare a bulk sample, however, small sizes of the resulting pellets and complexity of the pelletizer also severely restrict industrial application of this method [20]. Addition of a low-melting impurity with a melting temperature below 500 °C to the Sm₂Fe₁₇C_x 500 °C powder is another simpler method to prepare magnets with higher density. Eutectic Sm-based alloy [21] and Ce-Cu-Al hot-pressing alloy may be used as a binding agent [22]. Zn is most often used as a binding agent in this system to increase the coercive force of $Sm_2Fe_{17}N_x$ -based magnets and to reach $(BH)_{max}$ at the level of 200 kJ/m³ [23]. Meanwhile, exploring the relevant processes in the Sm-Fe-C system is also of interest.

In view of the aforesaid, it is important to investigate the zinc additive effect on formation of the structure and magnetic properties of $Sm_2Fe_{17}C_x$ -based powders. This study addressed the influence of low-temperature annealing

T _{ann} , °C	$Sm_2Fe_{17}C_x$, %	Zn, %	α-Fe, %	Sm ₂ O ₃ , %	Fe ₃ Zn ₁₀ , %	Sm ₂ Zn ₁₇ , %	$d_{\rm SFC}$, nm	$arepsilon_{ ext{SFC}},$ %	$V_{\rm SFC}$, Å ³	x, at./f.u.
25	82.0 ± 3.0	15.6 ± 0.5	2.4 ± 0.5	_	15.4 ± 1.4	0.8 ± 0.1	_	-	791.4 ± 0.6	0.26 ± 0.13
350 ± 10	55.1 ± 2.0	_	25.3 ± 0.9	12.3 ± 0.8	7.3 ± 1.1	_	8.9 ± 0.6	0.4 ± 0.1	819.4 ± 0.6	1.98 ± 0.22
375 ± 10	52.7 ± 1.8	_	27.2 ± 0.8	12.1 ± 0.7	8.0 ± 2.0	_	8.0 ± 0.5	0.6 ± 0.1	821.0 ± 1.2	2.08 ± 0.26
400 ± 10	49.0 ± 3.0	_	32.6 ± 0.8	11.1 ± 1.0	_	7.3 ± 1.0	11.3 ± 1.0	0.7 ± 0.1	822.4 ± 0.9	2.16 ± 0.25
450 ± 10	28.9 ± 1.8	_	35.6 ± 0.8	14.4 ± 0.6	_	21.1 ± 3.0	16.6 ± 2.5	0.4 ± 0.1	829.1 ± 1.2	2.57 ± 0.29

Table 1. X-ray diffraction spectra analysis data (d_{SFC} is the $Sm_2Fe_{17}C_x$ phase crystallite size; ε_{SFC} is the $Sm_2Fe_{17}C_x$ phase microstress; x is the carbon content in $Sm_2Fe_{17}C_x$, i.e. the amount of atoms per formula unit)

on formation of the structure and magnetic properties of $\rm Sm_2Fe_{17}C_x$ -based powders prepared by the mechanical synthesis from the $\rm Sm_2Fe_{17}$ alloy and carbon nanotubes with Zn additives. Moreover, a possibility to avoid the mechanical synthesis before annealing to prepare $\rm Sm_2Fe_{17}C_x$ (x>0.3) using carbon nanotubes as a carbon-containing additive was investigated.

2. Materials and methods

Sm-Fe alloy with Sm 24%, multiwall carbon nanotubes and metallic Zn were used as starting components. According to the X-ray diffraction data, the Sm-Fe alloy after homogenization contained only one Sm_2Fe_{17} (R $\bar{3}$ m) phase, then the homogenized alloy was triturated in a mortar and screened through a $50 \,\mu \text{m}$ sieve. Carbon nanotubes were added to the prepared alloy powder so that the amount of carbon atoms per formula unit of Sm₂Fe₁₇C_x is equal to 3 (x = 3): $Sm_2Fe_{17} + 3C = Sm_2Fe_{17}C_3$. The mixture was processed in the "Aktivator 2S" planetary mill (Novosibirsk, Russia) without using liquid and surfactants during 5 h at 400 rpm in Ar (99.9999%). Then Zn (15%) and heptane were added into the beakers in a glove box (with Ar) for further mixing in the planetary mill at 200 rpm during 5 min. The amount of Zn additive was chosen according to the literature data because sintering of Sm₂Fe₁₇N_x with 15 wt.the mixture was dried and passivated in Ar during 12h. For batch annealing, the powder was pressed and sealed in quartz tubes with Ar (0.3 bar, 99.998 %). Annealing was performed during 1 h at a heating rate of 15 K/min.

X-ray diffraction analysis was conducted using the Rigaku MiniFlex diffractometer (Tokio, Japan) by the Rietveld method implemented in PHAN% and SPECTRUM packages developed by the Department of Materials Physics of the MISIS University [25]. To determine the size of coherent scattering regions (CSR) and microdeformation level by X-ray line broadening, the Rietveld method was also used (instrumental broadening was considered using the LaB₆ standard). The amount of carbon atoms x per formula unit of $Sm_2Fe_{17}C_x$ was determined using a method described in [26].

Particle morphology was studied using the Tescan Vega3 SB scanning electron microscope (SEM) (Czech Republic) in a secondary electron recording mode at 20 kV.

Magnetic properties of samples were measured using the VSM-250 vibrating sample magnetometer (Changchun, China) at room temperature in fields up to 1600 kA/m.

3. Results and discussion

According to the X-ray diffraction analysis data (Figure 1, a, Table 1), the sample after grinding contained primarily the Sm₂Fe₁₇C_x phase (structural type R $\bar{3}$ m); 15% Zn (P6₃/mmc) and 2% α -Fe (Im3m) that were formed during grinding.

Carbon dissolution in the Sm_2Fe_{17} (R $\bar{3}$ m) phase is accompanied by insertion-type formation of a solid solution leading to an increase in the phase lattice constants and lattice cell volume; this effect may be used to determine the carbon content in the $Sm_2Fe_{17}C_x$ phase. Increase in the lattice cell volume of the $Sm_2Fe_{17}C_x$ phase up to 791 Å³ after grinding indicates poor dissolution of carbon during grinding (x = 0.26). X-ray line broadening analysis of the $Sm_2Fe_{17}C_x$ phase showed high ε_{SFC} in the order of 0.8%, which indicates that accumulation of crystalline structure defects occurred during grinding. Thus, mechanical synthesis, in particular, also includes power surface activation, which is a prerequisite for preparing $Sm_2Fe_{17}C_x$ with carbon concentration x > 0.3 even when carbon nanotubes are used as a carbon-containing additive instead of graphite [26]. To check whether the surface activation is necessary, a mixture of 50 µm of the Sm₂Fe₁₇ powder and carbon nanotubes was annealed without mechanical activation at 400 °C during 10 h and 20 h and additionally annealed at 500 °C during 5 h. Precision measurement of the Sm₂Fe₁₇ lattice constants was performed at each of the stages. It was shown that such processing didn't provide any significant change of $Sm_2Fe_{17}C_x$ lattice constants, the amount of atoms per formula unit after annealing was still x < 0.3.

According to the scanning electron microscopy data (Figure 2), after mechanical activation of the Sm₂Fe₁₇ and carbon nanotube mixture, particles with sizes in the order of units of nanometers had a near-equiaxed form and were gathered into agglomerates with sizes about tens of microns.

Annealing after mechanical activation led to the shift of $\mathrm{Sm_2Fe_{17}C_x}$ lines towards smaller angles (Figure 1, b-d) indicating that the lattice cell volume increased due to insertion-type dissolution of carbon. The change of the $\mathrm{Sm_2Fe_{17}C_x}$ lattice constants is associated exactly with

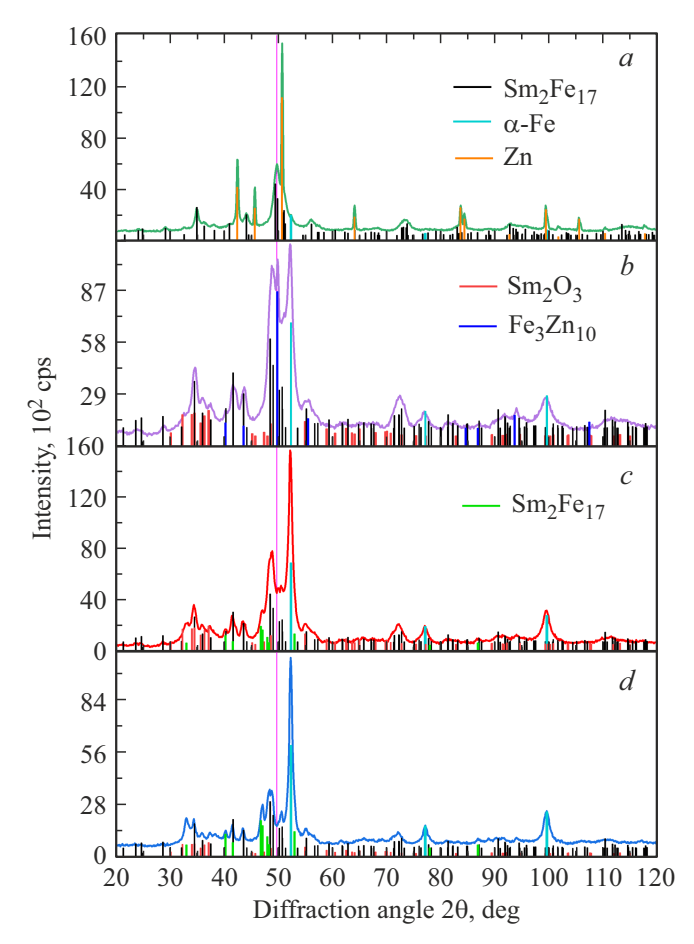


Figure 1. X-ray spectra of the samples: a) after grinding with Zn addition; after further annealing at: b) 350 °C, c) 400 °C, d) 450 °C.

carbon insertion, rather than with substitution of iron sites with zinc, because Zn solubility in this phase is minor — less than 0.2 atom per formula unit as reported in [27]. The amount of carbon atoms per formula unit of $\mathrm{Sm_2Fe_{17}C_x}$ increased to $x\approx 2$ after annealing at 350 °C and grew monotonously depending on the annealing temperature to $x\approx 2.6$ at 450 °C, which is close to the carbon solubility limit with similar synthesis methods [28].

X-ray line broadening analysis of the $Sm_2Fe_{17}C_x$ phase showed sudden decrease in the CSR size after annealing at 350 °C. This is explained by formation of new Fe_3Zn_{10} and Sm_2Zn_{17} phases, and by carbon diffusion at grain boundaries leading to chemical inhomogeneity: those crystallites that were closer to the grain boundary turned out to be carbon-enriched, while the crystallites in the center of grain still had the chemical composition Sm_2Fe_{17} . As the annealing temperature increased, the carbon diffusion path became longer, chemically homogeneous crystallites became larger and, consequently, the CSR size increased.

After annealing, formation of Zn-containing phases was observed: Fe₃Zn₁₀ (I4̄3m) and Sm₂Zn₁₇ (R3̄m) in the annealing temperature ranges of 350–375 and 400–450 °C, respectively. This process is associated with partial decomposition of the Sm₂Fe₁₇C_x (R3̄m) phase followed by formation of the α -Fe (Im3̄m) and Sm₂O₃ (C2/m) phases. According to the literature, iron release was also observed during annealing of the Sm₂Fe₁₇N_x and Zn mixture [29,30]. The most intense decomposition of the Sm₂Fe₁₇C_x phase was observed at the annealing temperature of 450 °C, while, in Zn-free annealing, the Sm₂Fe₁₇C_x phase actively disintegrated as early as at 400 °C [26]. This may suggest that Zn or Zn-containing phases affect the thermodynamic stability of Sm₂Fe₁₇C_x.

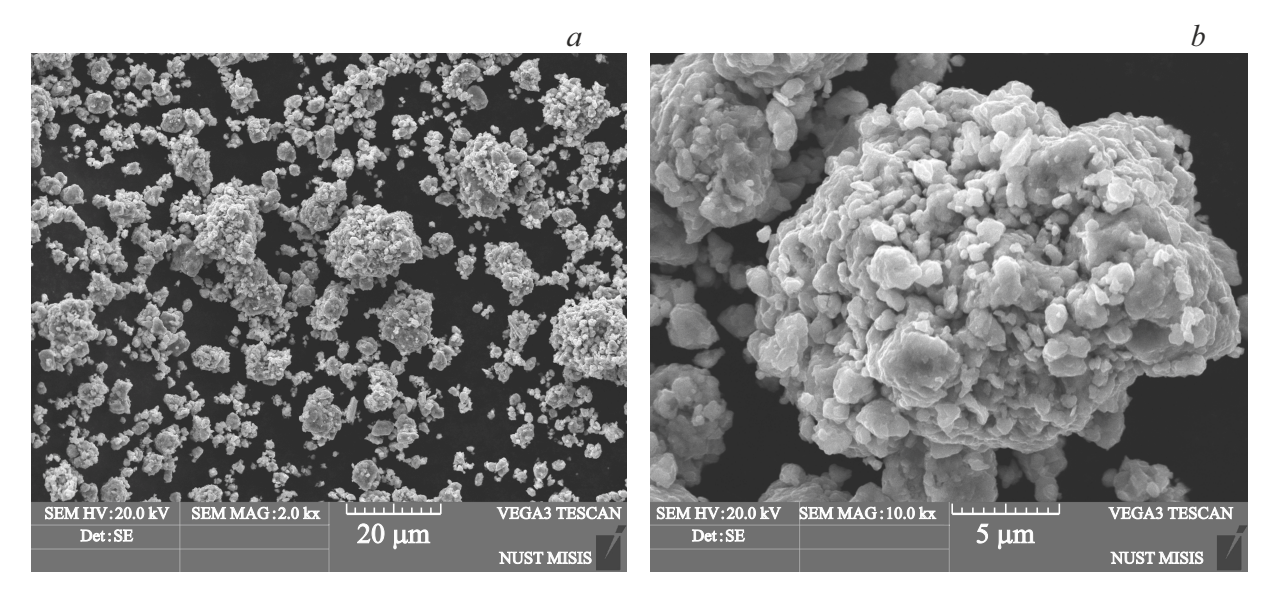


Figure 2. Microphotographs (SEM) of the powder after grinding.

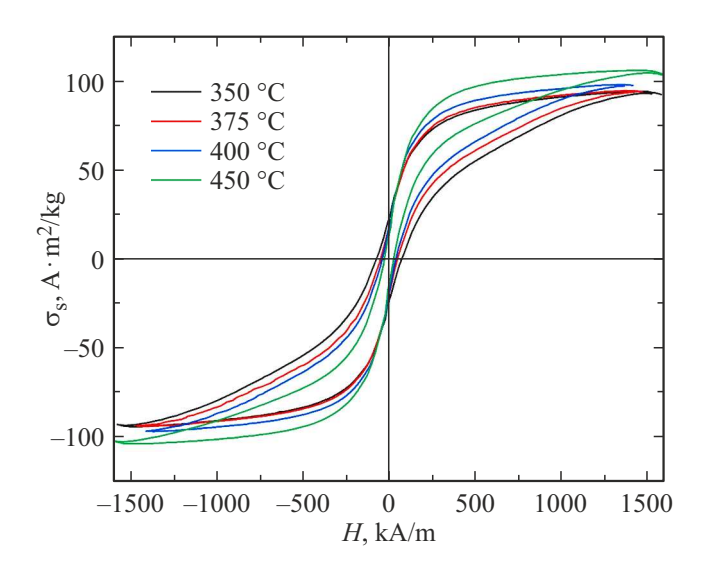


Figure 3. Magnetic hysteresis loops of annealed samples.

Table 2. Magnetic property measurements

T _{ann} , °C	H _c , kA/m	$\sigma_{\rm s}$, A·m ² /kg	$\sigma_{ m r}/\sigma_{ m s}$
350 ± 10	73.9 ± 2.2	95 ± 1	0.24
375 ± 10	49.2 ± 1.5	95 ± 1	0.19
400 ± 10	39.8 ± 1.2	98 ± 1	0.18
450 ± 10	26.7 ± 0.8	106 ± 2	0.13

Magnetic property measurements (Figure 3, Table 2) showed that, as the annealing temperature increased, the coercive force and squareness ratio σ_r/σ_s of the samples decreased monotonously, which is explained by monotonic decrease in the mass fraction of the magnetically hard phase $(Sm_2Fe_{17}C_x)$.

On the contrary, specific saturation magnetization increased monotonously as the annealing temperature increased, which is explained by the increase in the mass fraction of the magnetically soft α -Fe phase.

4. Conclusion

It is shown that carbon nanotubes used as a carbon-containing additive doesn't preclude the need for mechanical synthesis before annealing to prepare the $\mathrm{Sm_2Fe_{17}C_x}$ phase with high carbon concentration (x>0.3). Annealing within $350-375\,^{\circ}\mathrm{C}$ induces formation of the $\mathrm{Fe_3Zn_{10}}$ ($\mathrm{I\bar{4}3m}$) phase, while the $\mathrm{Sm_2Zn_{17}}$ ($\mathrm{R\bar{3}m}$) is formed at the annealing temperatures of $400-450\,^{\circ}\mathrm{C}$. When carbon nanotubes are used as a carbon-containing additive and Zn is added, intense decomposition of the $\mathrm{Sm_2Fe_{17}C_x}$ phase occurs at a higher annealing temperature ($450\,^{\circ}\mathrm{C}$) compared with Zn-free annealing ($400\,^{\circ}\mathrm{C}$). As the annealing temperature increases within $350-450\,^{\circ}\mathrm{C}$, the coercive force decreased monotonously from 74 to $26\,\mathrm{kA/m}$, and the specific saturation magnetization grew monotonously from 95 to

 $106 \,\mathrm{A\cdot m^2/kg}$, which was predominantly attributable to the release of the magnetically soft $\alpha\text{-Fe}$ phase.

Funding

This research was funded by Russian Science Foundation, grant number 23-73-00114.

Conflict of interest

The authors declare that they have no conflict of interest.

References

- [1] S. Boadu, E.A. Otoo. Renew. Sustain. Energy Rev. **191**, 114035 (2024). https://doi.org/10.1016/j.rser.2023.114035
- [2] J.P. Namahoro, Q. Wu, H. Su. Energy 278, Part A, 127869 (2023). https://doi.org/10.1016/j.energy.2023.127869
- [3] O. Summerfield-Ryan, S. Park. Ecol. Econ. **210**, 107841 (2023). https://doi.org/10.1016/j.ecolecon.2023.107841
- [4] L. Depraiter, S. Goutte. Resources Policy 86, *Part B*, 104137 (2023). https://doi.org/10.1016/j.resourpol.2023.104137
- [5] S. Liang, X. Shao, Y. Que, B. Guo, H. Bao, G. Tang, X. Yan, J. Bao, L. Yang, L. Qin, K. Shu, D. Chen, Z. Song. J. Alloys. Compd. 1003, 175689 (2024). https://doi.org/10.1016/j.jallcom.2024.175689
- [6] O.V. Zhdaneev, K.N. Frolov, V.A. Kryukov, V.A. Yatsenko. Mater. Sci. Energy Technol. 7, 107 (2024). https://doi.org/10.1016/j.mset.2023.07.007
- [7] V. Rallabandi, B. Ozpineci, P. Kumar. IEEE Spectrum 61, 8, 36 (2024). https://doi.org/10.1109/MSPEC.2024.10622061
- [8] B. Podmiljšak, B. Saje, P. Jenuš, T. Tomše, S. Kobe, K. Žušek,
 S. Šturm. Mater. 17, 4, 848 (2024).
 https://doi.org/10.3390/ma17040848
- [9] G.C. Hadjipanayis. J. Magn. Magn. Mater. 200, 1-3, 373 (1999). https://doi.org/10.1016/S0304-8853(99)00430-8
- [10] J.M.D. Coey, H. Sun. J. Magn. Magn. Mater. 87, 3, L251 (1990). https://doi.org/10.1016/0304-8853(90)90756-G
- [11] M. Katter, J. Wecker, C. Kuhrt, L. Schultz, R. Grössinger. J. Magn. Magn. Mater. 117, 3, 419 (1992). https://doi.org/10.1016/0304-8853(92)90099-A
- [12] L. Ye, F. Wang, Y. Liu, H. Zhou, L. Liu, Y. Ding, Y. Sun, A. Yan. J. Mater. Res. Technol. 30, 451 (2024). https://doi.org/10.1016/j.jmrt.2024.03.040
- [13] J. Takahashi, Y. Mitsui, M. Onoue, R. Kobayashi, K. Koyama. J. Magn. Magn. Mater. 554, 169295 (2022). https://doi.org/10.1016/j.jmmm.2022.169295.
- [14] Q. Fang, X. An, F. Wang, Y. Li, J. Du, W. Xia, A. Yan, J.P. Liu, J. Zhang. J. Magn. Magn. Mater. 410, 116 (2016). https://doi.org/10.1016/j.jmmm.2016.03.029
- [15] O. Mao, J.O. Ström-Olsen, Z. Altounian, J. Yang. J. Appl. Phys. 79, 8, 4619 (1996). https://doi.org/10.1063/1.361682
- [16] V.A. Mikheev, T.R. Nizamov, P.I. Nikolenko, A.V. Ivanova, A.I. Novikov, I.V. Dorofievich, A.S. Lileev, M.A. Abakumov, I.V. Shchetinin. Crystals 14, 12, 1028 (2024). https://doi.org/10.3390/cryst14121028
- [17] S.V. Seleznev, I.G. Bordyuzhin, T.R. Nizamov, V.A. Mikheev, M.A. Abakumov, I.V. Shchetinin. Inorg. Chem. Commun. 167, 112679 (2024). https://doi.org/10.1016/j.inoche.2024.112679
- [18] O. Mao, Z. Altounian, J. Yang, J.O. Ström-Olsen. J. Appl. Phys. 79, 8, 5536 (1996). https://doi.org/10.1063/1.362301

- [19] D.T. Zhang, M. Yue, J.X. Zhang. Powder Metall. 50, 3, 215 (2007). https://doi.org/10.1179/174329007X169128
- [20] I.V. Shchetinin, I.G. Bordyuzhin, R.V. Sundeev, V.P. Menushenkov, A.V. Kamynin, V.N. Verbetsky, A.G. Savchenko. Mater. Lett. 274, 127993 (2020). https://doi.org/10.1016/j.matlet.2020.127993
- [21] K. Otogawa, K. Takagi, T. Asahi. J. Alloys Compd. 746, 19 (2018). https://doi.org/10.1016/j.jallcom.2018.02.266
- [22] J. Zheng, S. Yu, H. Huang, R. Li, W. Cai, H. Chen, J. Li, L. Qiao, Y. Ying, W. Li, J. Yu, S. Che. Magnetochem. 8, 11, 149 (2022). https://doi.org/10.3390/magnetochemistry8110149
- [23] R. Matsunami, M. Matsuura, N. Tezuka, S. Sugimoto. J. Magn. Soc. Jpn. 44, 3, 64 (2020). https://doi.org/10.3379/msjmag.2005R003
- [24] D. Prabhu, H. Sepehri-Amin, C.L. Mendis, T. Ohkubo, K. Hono, S. Sugimoto. Scripta Materialia 67, 2, 153 (2012). https://doi.org/10.1016/j.scriptamat.2012.04.001
- [25] E.V. Shelekhov, T.A. Sviridova. Met. Sci. Heat Treat. **42**, 8, 309 (2000). https://doi.org/10.1007/BF02471306
- [26] V.A. Mikheev, I.G. Bordyuzhin, M.V. Gorshenkov, E.S. Savchenko, I.V. Dorofievich, I.V. Shchetinin. Metals. 14, 4, 472 (2024). https://doi.org/10.3390/met14040472
- [27] K. Hiraga, K. Okamoto, T. Iriyama. Mater. Trans. JIM 34, 6, 569 (1993). https://doi.org/10.2320/matertrans1989.34.569
- [28] C.N. Christodoulou, T. Takeshita. J. Alloys. Compd. **198**, *I* 2, 1 (1993). https://doi.org/10.1016/0925-8388(93)90137-C
- [29] K. Schnitzke, L. Schultz, J. Wecker, M. Katter. Appl. Phys. Lett. 57, 26, 2853 (1990). https://doi.org/10.1063/1.104202
- [30] C. Kuhrt, K. O'Donnell, M. Katter, J. Wecker, K. Schnitzke, L. Schultz. Appl. Phys. Lett. 60, 26, 3316 (1992). https://doi.org/10.1063/1.106678

Translated by E.Ilinskaya